A novel tRNA-derived small RNA, 5'tiRNA-Gln-TTG-001, aggravates cardiomyocyte inflammatory injury through upregulation of CLIC4

JING WANG, YINGCHUN YI, BO HAN, LI ZHANG and HAILIN JIA

Department of Pediatric Cardiology, Shandong Provincial Hospital Affiliated to Shandong First Medical University, Jinan, Shandong 250021, P.R. China

Received February 15, 2025; Accepted June 27, 2025

DOI: 10.3892/mmr.2025.13626

Abstract. Acute myocarditis encompasses a spectrum of diseases characterized by ongoing inflammation and cardiomyocyte injury, lacking specific diagnostic biomarkers and effective therapies. Transfer RNA (tRNA)-derived small RNAs (tsRNAs), formed by specific cleavage of tRNAs in response to certain stimuli, participate in diverse diseases; however, their involvement in myocarditis remains unclear. The present study aimed to investigate the role and mechanism of a novel tsRNA, 5'tRNA-derived stress-induced RNA (tiRNA)-Gln-TTG-001, in myocarditis. Plasma samples were obtained from patients with acute myocarditis to examine the clinical significance of 5'tiRNA-Gln-TTG-001. AC16 human cardiomyocytes treated with lipopolysaccharide to induce inflammatory responses were utilized to explore the function and mechanism of 5'tiRNA-Gln-TTG-001. Cell viability, apoptosis rates, and levels of factors associated with inflammation (IL-1β, IL-6 and IL-18), myocardial injury (creatine kinase MB and high-sensitivity cardiac troponin) and myocardial dysfunction (N-terminal pro-B-type natriuretic peptide) were quantified to assess the degree of cardiomyocyte inflammatory injury. RNA fluorescence *in situ* hybridization (RNA-FISH), cell transfection, dual-luciferase reporter assays and functional experiments, including gain-of-function and loss-of-function assays and rescue experiments, were carried out to further explore the underlying mechanisms. The results revealed that 5'tiRNA-Gln-TTG-001 was upregulated in acute myocarditis and positively correlated with high-sensitivity cardiac troponin T and T2 ratio. *In vitro* experiments demonstrated that 5'tiRNA-Gln-TTG-001 aggravated cardiomyocyte inflammatory injury. RNA-FISH revealed co-localization of 5'tiRNA-Gln-TTG-001 and chloride intracellular channel 4 (CLIC4) in the nucleus and cytoplasm. Gain-of-function and loss-of-function experiments revealed that 5'tiRNA-Gln-TTG-001 promoted CLIC4 expression. Dual-luciferase reporter assays indicated that 5'tiRNA-Gln-TTG-001 activated CLIC4 by binding to its 3'untranslated region. Furthermore, downregulation of CLIC4 rescued cardiomyocyte inflammatory injury aggravated by 5'tiRNA-Gln-TTG-001. Meanwhile, the knockdown of 5'tiRNA-Gln-TTG-001 reduced cardiomyocyte inflammatory injury and the effect was reversed by the upregulation of CLIC4. Overall, the present study demonstrated that 5'tiRNA-Gln-TTG-001 may aggravate cardiomyocyte inflammatory injury via CLIC4 upregulation. Moreover, 5'tiRNA-Gln-TTG-001 could offer a promising option for the diagnosis of myocarditis and serve as a potential therapeutic target.

Introduction

Acute myocarditis refers to a group of diseases characterized by sudden cardiomyocyte inflammatory injury, affecting 4-14 individuals per 100,000 per year worldwide (1). This condition disproportionately affects young, otherwise healthy individuals (2), and is associated with a mortality rate of 1-7% (1). Acute myocarditis is now understood to have various etiologies (infectious and non-infectious) and triggers a wide spectrum of signs or symptoms that are not specific to myocarditis. Laboratory findings include elevated high-sensitivity cardiac troponin (hs-CTnT), creatine kinase MB (CKMB) and N-terminal pro-B-type natriuretic peptide (NT-proBNP) levels, electrocardiographic ST-T segment changes and echocardiographic reduced left ventricular ejection fraction (LVEF). It is recommended to carry out cardiac magnetic resonance (CMR) or endomyocardial biopsy (EMB) to confirm the diagnosis (3-6); however, due to its invasive nature, risk of severe periprocedural complications and potential for sampling error, EMB is applicable only for selected patients (3,4,7-9). CMR enables a non-invasive, biopsy-like method to confirm the imaging features that indicate myocardial inflammation

Correspondence to: Professor Jing Wang, Department of Pediatric Cardiology, Shandong Provincial Hospital Affiliated to Shandong First Medical University, 324 Jingwu Road, Jinan, Shandong 250021, P.R. China
E-mail: wangjingsph@163.com

Key words: transfer RNA-derived small RNA, cardiomyocyte inflammatory injury, chloride intracellular channel 4, myocarditis, transfer RNA-derived stress-induced RNA

and injury (6). However, in a previous study, CMR detected myocarditis in 31.3% of juveniles and 57.9% of adults who had biopsy-proven myocarditis and was also less frequently carried out in patients with severe presentations (10). Thus, it is often challenging to establish a definitive diagnosis. While acute myocarditis resolves in ~50% of cases within the first 2-4 weeks (3), it can progress to dilated cardiomyopathy (DCM) in susceptible individuals, a condition characterized by dilated heart chambers, decreased myocardial contractility and arrhythmia. The prevalence of biopsy-confirmed myocarditis among patients with DCM is reported to range from 9-46%, depending on study populations (3). Currently, first-line therapy options for myocarditis are largely empirical and supportive, exhibiting limited ability to reverse or prevent disease progression (1-4,7,9). Thus far, myocarditis remains a challenging clinical issue lacking specific diagnostic biomarkers and effective therapies.

Transfer RNA (tRNA)-derived small RNAs (tsRNAs) represent a novel class of small non-coding RNAs produced by the selective and specific cleavage of mature or precursor tRNAs, and can be categorized into tRNA-derived stress-induced RNAs (tiRNAs; 28-36 nucleotides) and tRNA-derived fragments (15-32 nucleotides) based on their cleavage sites and lengths (11). tiRNAs are further divided into 3'-tiRNA and 5'-tiRNA, derived from the 3'-terminal and 5'-terminal regions, respectively. Notably, tsRNAs have long considered to be random degradation byproducts of tRNAs; however, increasing evidence suggests that they have potential biological functions and are essential for cellular homeostasis as well as adaption to changing conditions (12,13). tsRNAs have also been identified as differentially expressed in various pathological processes and diseases, such as infectious, autoimmune and neurodegenerative diseases, and several types of cancer (14-18). Several dysregulated plasma tsRNAs have also been revealed to associate with the extent or severity of epilepsy (19), indicating their stability and specificity as potential biomarkers and therapeutic targets. Our prior study established comprehensive expression profiles of plasma tsRNAs in fulminant myocarditis (FM), a type of acute myocarditis, for the first time (20). Nevertheless, the intricate mechanistic roles of tsRNAs in the onset and advancement of acute myocarditis have yet to be thoroughly investigated.

Chloride intracellular channel 4 (CLIC4), part of the CLIC protein family, is abundantly expressed in the heart (21), is a key regulator of apoptosis (22-24) and a key mediator of inflammation (25). CLIC4 serves an important role in various diseases (24,26); however, the upstream regulatory mechanisms of CLIC4 and its role in the pathogenesis of myocarditis remain poorly understood.

Our previous study identified 5'tiRNA-Gln-TTG-001 as a potential diagnostic marker associated with myocarditis onset and progression, with CLIC4 as a potential target (20). Based on these findings, the present study aimed to elucidate whether 5'tiRNA-Gln-TTG-001 could act as a novel plasma biomarker for the early and accurate detection of acute myocarditis and to assess its involvement in the development and progression of acute myocarditis through CLIC4. Elucidating the underlying molecular mechanisms mediated by tsRNAs may help to develop new therapeutic approaches for patients with this disease.

Materials and methods

Patients. Study participants were recruited from the Department of Pediatric Cardiology, Shandong Provincial Hospital Affiliated to Shandong First Medical University (Jinan, China) over a 3-year period, from September 2018 to September 2021. The cohort comprised three groups: Juveniles with FM (n=20), age- and sex-matched healthy controls (n=20), and age- and sex-matched patients with DCM with decompensated heart failure as disease controls (n=20). Peripheral blood samples (3-5 ml) were obtained from all study participants. As for the FM group, the first samples were taken during the acute phase just before treatment initiation (FM-A group), and the second blood samples were collected during the convalescent phase when they could be discharged (FM-C group). Patients with FM were diagnosed based on the current guidelines (3), with further confirmation by CMR (5,6).

The inclusion criteria were defined as follows: <18 years of age; rapid collapse of hemodynamic status following a fatal course, such as acute heart failure, life-threatening arrhythmias, cardiogenic shock or aborted sudden death within a 2-week timeframe; no coronary artery disease and other identifiable etiologies; the presence of positive necrosis biomarkers, such as hs-CTnT; meeting at least two of the three CMR criteria for acute myocarditis as defined by the Lake Louise Criteria (5). The exclusion criteria included: Conditions that pose a threat to life, excluding those attributable to FM; pre-existing cardiovascular diseases or extracardiac conditions that may explain the syndrome (such as valvular heart disease, congenital heart defects or hyperthyroidism); prior administration of immunomodulatory therapies before the initial sample collection; individuals who either succumbed or opted out of treatment prior to reaching clinical stabilization.

All patients diagnosed with FM underwent comprehensive pathogen screening to identify the presence of the following infectious agents: Coxsackievirus, cytomegalovirus, Epstein-Barr virus, rubella, herpes simplex virus-2, parvovirus B19, human herpesvirus 6, respiratory syncytial virus, parainfluenza viruses, influenza A virus, influenza B virus, human adenovirus, rhinovirus, hepatitis A virus, hepatitis B virus, hepatitis C virus, hepatitis E virus, human immunodeficiency virus, *Treponema pallidum* (syphilis), group A *Streptococcus*, *Mycoplasma pneumoniae* and *Chlamydia pneumoniae*. Additionally, blood and sputum cultures were conducted to further investigate potential infections. Written informed consent was obtained from the legal guardians of each participant in accordance with The Declaration of Helsinki. The institutional Ethics Committee of Shandong Provincial Hospital Affiliated to Shandong First Medical University (Jinan, China) approved the present study (approval no. 2018-115).

Culture conditions and induction of the cardiomyocyte inflammatory injury model. AC16 human cardiomyocytes isolated from normal human ventricular tissue were obtained from the BeNa Culture Collection; Beijing Beina Chunglian Institute of Biotechnology, and cultured under standard conditions in Dulbecco's Modified Eagle's Medium (DMEM; Gibco; Thermo Fisher Scientific, Inc.) supplemented with 10% fetal bovine serum (Gibco; Thermo Fisher Scientific, Inc.) at

37˚C in a humidified incubator with 5% CO_2. AC16 cells were initially cultured under standard conditions for 24 h and subsequently incubated in serum-free DMEM for an additional 12 h. The cells were treated with 40 μg/ml lipopolysaccharide (LPS; MilliporeSigma) at room temperature for 36 h. The control group was administered physiological saline instead of LPS. Following this treatment, AC16 cells were washed with PBS, digested with 0.25% trypsin and collected by centrifugation at 1,000 x g for 5 min at room temperature, and their cell culture supernatants (CCS) were collected using a pipette.

Pretreatment. Blood samples were processed within 1 h of collection. They underwent centrifugation at 1,900 x g for 10 min at 4˚C, and the top plasma layer was transferred to a different conical tube. Subsequently, the top plasma layer was subjected to a second centrifugation at 16,000 x g for 10 min at 4˚C, after which the supernatant was collected for RNA extraction and stored in aliquots at -80˚C. CCS samples intended for RNA extraction underwent centrifugation at 3,000 x g for 15 min at 4˚C, whereas those for ELISA were centrifuged at 1,000 x g for 20 min at 4˚C.

Target prediction for 5'tiRNA-Gln-TTG-001 candidates. Identification of the predicted target mRNAs of 5'tiRNA-Gln-TTG-001 may provide the basis for understanding the functions of 5'tiRNA-Gln-TTG-001. Thus, candidate target genes of 5'tiRNA-Gln-TTG-001 were analyzed and CLIC4 was selected as a candidate target based on target gene prediction scores using online tools (Diana Tools MR-microT; https://mrmicrot.imsi.athenarc.gr/?r=mrmicrot/index), as well as Kyoto Encyclopedia of Genes and Genomes (https://www.genome.jp/entry/K05024) and Gene Ontology (https://amigo.geneontology.org/amigo/term/GO:0005247) analyses.

RNA extraction. Total sRNAs were extracted from 200 μl pre-processed plasma and CCS using miRNeasy Serum/Plasma Kit (Qiagen GmbH) according to the manufacturer's protocol. To ensure RNA purification efficiency and normalization, 3 μl synthetic cel-miR-39-3p (20 fmol/μl; Guangzhou RiboBio Co., Ltd.) was added as a spike-in control. An Agilent 2100 Bioanalyzer (Agilent Technologies Inc.) was used to evaluate the concentration and quality of the extracted sRNAs through absorbance spectrometry. Total RNAs and sRNAs were extracted from AC16 cells using AG RNAex Pro RNA (Hunan Accurate Bio-Medical Technology Co., Ltd.) and RNAiso for Small RNA (Takara Bio, Inc.), respectively, according to the instructions provided by the manufacturers. A NanoDrop™ 2000 spectrophotometer (Thermo Fisher Scientific, Inc.) was used to evaluate the concentration and purity of the extracted RNAs.

Reverse transcription-quantitative PCR (RT-qPCR) validation. sRNAs from pretreated plasma or CCS and AC16 cells were converted into cDNA using Taqman microRNA (miRNA) cDNA synthesis kits (Serum/Plasma) and Taqman miRNA cDNA synthesis kits (Haigene Biotech Co., Ltd.). According to the manufacturer's protocol, 10 μl sRNA extracted from pretreated plasma or CCS was initially combined with 2.5 μl 5X TaqMan miRNA RT Solution A and incubated for 30 min at 37˚C, followed by 5 min at 85˚C. Thereafter, the resulting 12.5-μl reaction mixture was combined with 2.5 μl 10X PS TaqMan miRNA RT Primer, 2.5 μl 10X TaqMan miRNA RT Solution B and 7.5 μl double-distilled water. Finally, this 25-μl reaction mixture was incubated sequentially for 5 min at 30˚C, 60 min at 55˚C and 5 min at 95˚C to synthesize cDNA. For sRNAs from AC16 cells, a similar process was followed with adjusted volumes; 4 μl sRNA was initially combined with 1 μl 5X TaqMan miRNA RT Solution A and subsequently incubated for 30 min at 37˚C, followed by 5 min at 85˚C. Thereafter, the resulting 5-μl reaction mixture was combined with 2 μl 10X PS TaqMan miRNA RT Primer, 2 μl 10X TaqMan miRNA RT Solution B and 11 μl double-distilled water. Finally, this 20-μl reaction mixture was incubated sequentially for 5 min at 30˚C, 60 min at 55˚C and 5 min at 95˚C to synthesize cDNA. According to the instructions provided by the manufacturer, these cDNAs were quantified using Taqman RT-qPCR mix (Haigene Biotech Co., Ltd.), which includes 5X golden HS Taqman RT-qPCR mix and 20X miRNA Taqman assay, via qPCR. The qPCR reactions were carried out in a 20-μl volume, comprising 2 μl cDNA (diluted 1:10 for cellular cDNA), 4 μl 5X golden HS Taqman RT-qPCR mix, 1 μl 20X miRNA Taqman assay and 13 μl double-distilled water. The amplification process began with initial denaturation at 95˚C for 15 min, followed by 45 cycles carried out for 10 sec at 95˚C and 60 sec at 60˚C. Synthetic cel-miR-39-3p (20 fmol/μl; Guangzhou RiboBio Co., Ltd.) served as a spike-in control for tsRNAs from plasma and CCS samples. In the case of tsRNAs from AC16 cells, U6 was utilized as the internal reference gene. Evo M-MLV RT Premix for qPCR (Hunan Accurate Bio-Medical Technology Co., Ltd.) was used to convert total RNA extracted from AC16 into cDNA. According to the manufacturer's protocol, total RNA was combined with 2 μl 5X Evo M-MLV RT Master Mix and RNase-Free water to comprise a 10-μl reaction system, and was subsequently incubated for 15 min at 37˚C, followed by 15 sec at 85˚C to obtain cDNA. According to the manufacturer's instructions, the cDNA generated was quantified by qPCR using the SYBR® Green Premix Pro Taq HS qPCR Kit (Hunan Accurate Bio-Medical Technology Co., Ltd.). A 20-μl qPCR reaction volume was prepared, comprising 2 μl cDNA, 10 μl 2X SYBR Green Pro Taq HS Premix, 0.4 μl each forward and reverse primer (10 μM) and 7.2 μl double-distilled water, with GAPDH serving as the internal reference. The relative expression levels were calculated using the $2^{-\Delta Cq}$ and $2^{-\Delta\Delta Cq}$ methods (27). The PCR primer sequences (in 5'-3' direction) were as follows: Toll-like receptor 4 (TLR4), forward TGG TGTCCCAGCACTTCATC, reverse CTGTCCTCCCAC TCCAGGTA; lymphocyte antigen 96 (LY96), forward ATT TGCCG AGGATCTGATGACG, reverse TTGTTGTATTCA CAGTCTCTCCCT; RelA, forward TGAACCAGGGCATAC CTGTG, reverse CCCCTGTCACTAGGCGAGTT; NF-κB1, forward ATGTGGGACCAGCAAAGGTT, reverse CAC CATGTCCTTGGGTCCAG; IL-1β, forward CTTCTGGGA AACTCACGGCA, reverse AGCACACCCAGTAGTCTT GC; IL-6, forward TGAGGAGA CTTGCCTGGTGAA, reverse CAGCTCTGGCTTGTTCCTCAC; IL-18, forward ATTGACCAAGGAAATCGGCCTC, reverse GGTCCG GGGTGCATTATCTCT; CLIC4, forward GAGGAC AAAGAGCCCCTCAT, reverse AAGGGGCAGTTTCCT

Table I. RNA fluorescence *in situ* hybridization probe sequences.

Probe	Sequence
5'tiRNA-Gln-TTG-001	5'-Cy3-TCTCCGTGCCACCTATCACACCCCATCCTA-3'
CLIC4-1	5'- FAM-CCCATTCAGCGGCATCGACAACG-3'
CLIC4-2	5'-FAM-AATTTGGCAAAGATGTCCATTCCAGC-3'
CLIC4-3	5'- FAM-TGCCATCCAGAAATTTACGTGTAGA-3'
18S	5'-FAM-CTGCCTTCCTTGGATGTGGTAGCCGTTTC-3'
NC	5'-FAM-TGCTTTGCACGGTAACGGTAACGCCTGTTTT-3'

CLIC4, chloride intracellular channel 4; Cy3, cyanine 3; FAM, carboxyfluorescein; siRNA, small interfering RNA; tiRNA, transfer RNA-derived stress-induced RNA. CLIC4-1, CLIC4-2, and CLIC4-3 were used the same time in FISH analysis.

ATGCT T; GAPDH, forward GCACCGTCAAGGCTGAGA AC, reverse TGGTGAAGACGCCAGTGGA.

RNA fluorescence in situ hybridization (RNA-FISH) probes. Probes targeting 5'tiRNA-Gln-TTG-001, CLIC4 and 18S rRNA were designed and produced by Shanghai GenePharma Co., Ltd. with the sequences listed in Table I. A cyanine 3-labeled probe (red) was designed to visualize the distribution of 5'tiRNA-Gln-TTG-001. A carboxyfluorescein-labeled probe (green) was used to visualize the distribution of CLIC4 and ribosomal RNA (18S). 18S was used as a cytoplasmic sRNA control, a nonsense sequence was applied as the negative control (NC) to exclude non-specific staining and DAPI (blue) was used to counterstain the nucleus. The probe signals were detected using an RNA-FISH Kit (catalogue nos. F12101 and F12201; Shanghai GenePharma Co., Ltd.), which contains Buffers A, C, E and F. AC16 cells were introduced into 24-well culture plates with cell-climbing slices at a density of $2x10^4$ cells/well and cultured to 50-70% confluence. Subsequently, the medium was removed, and the cells were gently rinsed twice with PBS for 5 min each. After removing the PBS, 200 μl 4% paraformaldehyde was added per well to fix the cells at room temperature for 15 min. Following the removal of paraformaldehyde, 200 μl freshly prepared 0.1% Buffer A was added per well, and the cells were incubated at room temperature for 15 min. Buffer A was then removed, and the cells were gently rinsed twice with PBS for 5 min each. During this period, two concurrent processes were conducted. The first process involved incubating Buffer E alone in a 73˚C water bath for 30 min until it became clear and transparent following the first wash in PBS. Subsequently, a mixture comprising 196 μl incubated Buffer E and 4 μl probe was prepared and denatured at 73˚C for 5 min in the dark. The second process entailed the addition of 200 μl 2X Buffer C to each well following the removal of PBS after the second wash, and the cells with Buffer C were then incubated at 37˚C for 30 min. Consequently, this approach allowed for the simultaneous preparation of the denatured probe mixture (196 μl Buffer E and 4 μl probe) and the incubation of cells in Buffer C. Subsequently, Buffer C was removed from the cells and 200 μl denatured probe mixture was added per well for overnight hybridization at 37˚C in the dark. The following day, the samples were removed from the 37˚C incubator, the probe mixture was discarded, and each well was washed with 200 μl 0.1% Buffer F, preheated to 42˚C for 5 min. After removing Buffer F, each well was washed with 200 μl 2X Buffer C, also preheated to 42˚C for 5 min. Buffer C was then removed, and each well was washed with 200 μl 1X Buffer C, preheated to 42˚C for 5 min. Subsequently, 200 μl DAPI was added to each well and incubated in the dark for 20 min at room temperature to stain the nuclei. After DAPI was removed, and the cells were gently rinsed twice with PBS for 5 min each. Subsequently, an anti-quenching agent was added to a clean glass slide, then the coverslip with the cells facing downward was positioned onto the slide and observed using a fluorescence microscope (BX63; Olympus Corporation).

Cell transfection. AC16 cells were cultured in 6-well plates until they reached 70-90% confluence prior to transfection according to the experimental protocol. Mimics for 5'tiRNA-Gln-TTG-001 and mimics NC [final concentration, 50 nM; Genomeditech (Shanghai) Co., Ltd.], inhibitors for 5'tiRNA-Gln-TTG-001 and inhibitor NC [final concentration, 100 nM; Genomeditech (Shanghai) Co., Ltd.], CLIC4 siRNA and siRNA NC [final concentration, 100 nM; Genomeditech (Shanghai) Co., Ltd.], and CLIC4 overexpression plasmid [pCDNA3.1(+); final concentration, 25 nM; Genomeditech (Shanghai) Co., Ltd.] and CLIC4 NC [final concentration, 25 nM; Genomeditech (Shanghai) Co., Ltd.] were diluted in 125 μl Opti-MEM® reduced serum medium (Gibco; Thermo Fisher Scientific, Inc.). Subsequently, 5 μl P3000™ transfection reagent (Thermo Fisher Scientific, Inc.) was added to each diluted mixture to create a master mix. In parallel, 125 μl Opti-MEM reduced serum medium was used to dilute 5 μl Lipofectamine® 3000 reagent (Invitrogen; Thermo Fisher Scientific, Inc.). The master mix was subsequently combined with the diluted Lipofectamine 3000 reagent and left to incubate at room temperature for 10-15 min. Finally, 100 μl of the mixture was introduced to the cells at room temperature. The cell plate was gently agitated to ensure even distribution, after which it was placed in a 37˚C cell incubator for 48 h. A total of 24 h post-transfection, the cells were used for subsequent experiments. The sequences were as follows: 5'tiRNA-Gln-TTG-001 mimics, sense, 5'-UAGGAUGGGGUGUGAUAGGUGGCA CGGAGAAUUU-3', and antisense, 5'-AUCCUACCCCACACU AUCCACCGUGCCUCUUAAA-3'; 5'tiRNA-Gln-TTG-001 mimics NC, sense, 5'-UCACAACCUCCUAGAAAGAGU AGA-3', and antisense, 5'-AGUGUUGGAGGAUCUUUC UCAUCU-3'; 5'tiRNA-Gln-TTG-001 inhibitor, 5'-AAA

UUCUCCGUGCCACCUAUCACACCCCAUCCUA-3'; 5'tiRNA-Gln-TTG-001 inhibitor NC, 5'-UCUACUCUUUCU AGGAGGUUGUGA-3'; CLIC4 siRNA, sense, 5'-GAAAUG ACAUUAGCUGAUU-3', and antisense,5'-CUUUACUGU AAUCGACUAA-3'; CLIC4siRNA NC, sense, 5'-UUCUCC GAACGUGUCACGU-3', and antisense, 5'-AAGAGGCUU GCACAGUGCA-3'.

Cell counting kit-8 (CCK-8) assays. Both normal and transfected cells were seeded at a concentration of 2,000 cells/well in the middle section of a 96-well plate. The cells underwent the aforementioned treatment to induce inflammatory injury following an overnight incubation period. After incubating for 36 h, 10 μl CCK-8 solution (Dojindo Laboratories, Inc.) was introduced to each well. Following a 75-min incubation at 37˚C, absorbance values were measured at 450 nm using a microplate reader (EL340; Agilent Technologies, Inc.). Cell viability, measured as the survival rate of cells, was determined by setting the control cell survival to 100%.

Annexin V-phycoerythrin (PE)/7-aminoactinomycin D (AAD) double staining combined with flow cytometry. Apoptosis was measured using flow cytometry with Annexin V-PE and7-AAD double staining, according to the guidelines provided by BD Biosciences. The cells were collected by centrifugation at 900 x g for 5 min at room temperature, rinsed three times with 1X phosphate-buffered saline, and stained with Annexin V-PE/7-AAD for 15 min at room temperature in the dark. The analysis of groups of 20,000 cells was conducted using a BD LSRFortessa™ flow cytometer (BD Biosciences) and data were analyzed using FlowJo version 10.8.1 (BD Biosciences).

ELISA. CCS collected for ELISA was subjected to centrifugation at 1,000 x g for 20 min at 4˚C. Subsequently, the concentrations of IL-1β, IL-6, IL-18, cTnT, CKMB and NT-proBNP were quantified using commercially available ELISA kits (IL-1β ELISA, cat. no. VAL101, R&D Systems, Inc.; IL-6 ELISA, cat. no. VAL102C, R&D Systems, Inc.; IL-18 ELISA, cat. no. VAL131, R&D Systems, Inc.; cTnT ELISA, cat. no. E-EL-H0646, Elabscience Bionovation Inc.; CKMB ELISA, cat. no. E-EL-H1434, Elabscience Bionovation Inc., NT-proBNP ELISA, cat. no. E-EL-H6126, Elabscience Bionovation Inc.) according to the manufacturers' protocols. The absorbance was measured at 450 nm with a microplate reader (EL340; BioTek; Agilent Technologies, Inc.).

Dual-luciferase reporter assays. The 3'-untranslated region (3'UTR) of CLIC4 was produced and inserted into luciferase reporter vectors [Genomeditech (Shanghai) Co., Ltd.], creating constructs containing the wild-type [CLIC4 WT, pGL3-CMV-LUC-H_CLIC4 3'UTR(tiRNA-Gln-TTG-001) WT, Genomeditech (Shanghai) Co., Ltd.], and a mutant 5'tiRNA-Gln-TTG-001 binding site [CLIC4 MT, pGL3-CMV-LUC-H_CLIC4 3'UTR (tiRNA-Gln-TTG-001) MT, Genomeditech (Shanghai) Co., Ltd.] An empty plasmid served as a NC [CLIC4 NC, pGL3-CMV-LUC-MCS, Genomeditech (Shanghai) Co., Ltd.]. These plasmids were transfected into 293 cells (The Cell Bank of Type Culture Collection of The Chinese Academy of Sciences), in combination with 5'tiRNA-Gln-TTG-001 mimics or tiRNA mimics NC, which were then cultured for 24 h at 37˚C and harvested 48 h post-transfection to detect the luciferase activities. The *Renilla* luciferase (Rluc) and firefly luciferase (Luc) sequences were cloned into the pGL3-CMV-LUC-MCS. Luc and Rluc activities were assessed using the Dual Luciferase Reporter Gene Assay Kit [cat. no. GM-040502A; Genomeditech (Shanghai) Co., Ltd.], and the Luc activity was normalized to Rluc activity to obtain relative luciferase activity (Luc/Rluc).

Statistical analysis. Each experiment was conducted independently in at least triplicate. Continuous data are presented as the mean ± standard deviation, whereas non-parametric data are presented as median and interquartile range. R programming language (version 3.5.3) (28) and SPSS v.24.0 (IBM Corp.) software was used for statistical analyses. For data visualization, the R programming language (version 3.5.3) and GraphPad Prism 8.0 (Dotmatics) were utilized. Paired-sample t-tests, and independent-sample t-tests were used for comparisons between two groups, and one-way analysis of variance with Tukey's post hoc test. was used for comparisons of multiple groups. The statistical dependence between the rankings of two variables was measured using the Spearman rank correlation coefficient. $P<0.05$ was considered to indicate a statistically significant difference.

Results

Upregulation of 5'tiRNA-Gln-TTG-001 in acute myocarditis and correlation with clinical parameters. Building on our previous study, which showed the upregulation of plasma 5'tiRNA-Gln-TTG-001 in FM (20), plasma 5'tiRNA-Gln-TTG-001 expression levels were examined in a larger sample size, including 20 FM cases and 20 age- and sex-matched healthy controls. Table II provides a detailed overview of the clinical presentations and examination findings for these patients. Consistent with our previous results, 5'tiRNA-Gln-TTG-001 expression levels were markedly elevated in acute myocarditis (FM-A) compared with control samples (CON; Fig. 1A). To assess the diagnostic potential of 5'tiRNA-Gln-TTG-001 as a biomarker for acute myocarditis, blood samples were collected during the convalescent phase. Analysis revealed a marked decrease in 5'tiRNA-Gln-TTG-001 expression levels during the convalescent phase (FM-C) compared with the acute phase (FM-A; Fig. 1B). Furthermore, the expression levels of 5'tiRNA-Gln-TTG-001 were compared with clinical parameters associated with myocarditis obtained from the hospital medical records, which include peripheral blood indices such as inflammatory markers [white blood cell count, neutrophil ratio, C-reactive protein, procalcitonin and erythrocyte sedimentation rate], myocardial injury markers (CKMB mass and hs-CTnT), myocardial dysfunction markers (NT-proBNP), LVEF and CMR data, including early gadolinium enhancement rate and T2 ratio. Analysis revealed a positive correlation between 5'tiRNA-Gln-TTG-001 expression levels and hs-cTnT ($R=0.785$; Fig. 1C) or T2 ratio ($R=0.7118$; Fig. 1D). Expression of 5'tiRNA-Gln-TTG-001 demonstrated no significant correlation with other clinical parameters (Fig. 1E-M). The relationship between patients with different pathogens was not compared because the number of pathogen-positive patients was insufficient. To

Table II. Baseline clinical characteristics of patients with fulminant myocarditis (n=20).

Characteristic	Value
Male, n (%)	14 (70%)
Age, years	10.53±3.93
Clinical presentation, n (%)	
Fever	13 (65%)
Emesis	8 (40%)
Chest pain	6 (30%)
Headache	4 (20%)
Fatigue	4 (20%)
Convulsion	4 (20%)
Breath shortness	3 (15%)
Abdominal pain	3 (15%)
Abdominal distention	2 (10%)
Amaurosis	1 (5%)
Syncope	1 (5%)
Physical examinations	
SBP, mmHg[a]	79.50 (75.00, 85.50)
DBP, mmHga	46.58±10.99
HR, bpm	78.80±34.90
Temperature, ˚C	37.55 (36.63, 38.50)
Laboratory findings	
Pathogen, n (%)	20 (100%)
Positive	9 (45%)
Negative	11 (55%)
Leucocytes, 10^9/l	9.58 (7.6, 15.29)
Neutrophils, %)	77.45±11.37
ESR, mm/h[b]	11.5 (3.75,21.25)
CRP, mg/l	20.17 (5.38, 54.95)
PCT, ng/ml	0.18 (0.09, 0.52)
Peak hs-cTnT, pg/ml	1,749 (915.25, 3,700.25)
Peak CKMB mass, ng/ml	33.41 (10.43, 61.08)
Peak NT-proBNP, pg/ml	10,950.5 (2,023.75, 18,899.00)
ECG at admission, n (%)	
CAVB during myocarditis	9 (45%)
ST segment elevation	8 (40%)
T wave inversion	4 (20%)
PVC	1 (5%)
Non-sustain VT	2 (10%)
PAC	1 (5%)
Sinus bradycardia	1 (5%)
Chest X-ray	
Enlarged heart shadow, n (%)	10 (50%)
Pulmonary edema, n (%)	11 (55%)
Pleural effusion, n (%)	3 (15%)
Pneumonia, n (%)	6 (30%)
Atelectasis, n (%)	1 (5%)
Cardiothoracic ratio	0.51 (0.44,0.58)
Echocardiographic parameters at admission	
Dilated LVEDD, n (%)	9 (45%)
LVEF, %	39.40±10.51
Pericardial effusion, n (%)	8 (40%)
Decreased wall motion, n (%)	20 (100%)
CMR at admission	
EGEr, %	4.20±0.23
T2 ratio, %	2.01±0.19
LGE, n (%)	14 (70%)
CCTA performed, n (%)	20 (100%)
Days in hospital	18.5 (15.25,27.5)
Treatments in-hospital, n (%)	
γ-globulin	20 (100%)
ECMO	6 (30%)
Ventilator	5 (25%)
Temporary pacemaker	8 (40%)
Hemofiltration	1 (5%)

[a]Values of blood pressure of 8 juveniles were too low to measure. [b]ESR detected in 10 juveniles. Continuous variables are expressed as mean ± standard deviation for normally distributed variables, and median and interquartile range for non-normally distributed variables. CAVB, complete atrioventricular block; CCTA, coronary computed tomography angiography; CKMB, creatin kinase MB; CRP, C-reactive protein; DBP, diastolic blood pressure; ECMO, extracorporeal membrane oxygenation; EGEr, early gadolinium enhancement ratio; ESR, erythrocyte sedimentation rate; HR, heart rate; hs-cTnT, high-sensitivity cardiac troponin T; LGE, late gadolinium enhancement; LVEDD, left ventricular end-diastolic diameter; LVEF, left ventricular ejection fraction; NT-pro BNP, N-terminal pro-B-type natriuretic peptide; PAC, premature atrial contraction; PCT, procalcitonin; PVC, premature ventricular contraction; SBP, systolic blood pressure; VT, ventricular tachycardia.

explore the diagnostic specificity of 5'tiRNA-Gln-TTG-001 as a biomarker for acute myocarditis, 5'tiRNA-Gln-TTG-001 expression levels between patients with FM and 20 age- and sex-matched patients with decompensated heart failure due to DCM (HF-CON) were compared. Analysis revealed that 5'tiRNA-Gln-TTG-001 expression levels were significantly elevated in acute myocarditis (FM-A) compared with DCM (HF-CON; Fig. 1N). No significant differences were observed between FM-C, CON and HF-CON (Fig. 1O). Collectively, the aforementioned findings indicate that 5'tiRNA-Gln-TTG-001 could function as an innovative biomarker for diagnosing acute myocarditis.

Synthesis and localization of 5'tiRNA-Gln-TTG-001 in cardiomyocytes. To determine whether 5'tiRNA-Gln-TTG-001 is synthesized and secreted by cardiomyocytes, sRNAs were extracted from AC16 cells and their CCS for RT-qPCR assays. Analysis revealed the presence of 5'tiRNA-Gln-TTG-001 in both AC16 cells (Fig. 2A) and CCS (Fig. 2B), indicating that cardiomyocytes could synthesize and secrete 5'tiRNA-Gln-TTG-001. The subcellular localization of 5'tiRNA-Gln-TTG-001 was further detected using RNA-FISH. As shown in Fig. 2C, red fluorescence (5'tiRNA-Gln-TTG-001 probe) was observed in both the nucleus and cytoplasm of cardiomyocytes. By contrast, green fluorescence (18S rRNA probe) was confined to the cytoplasm, and blue fluorescence

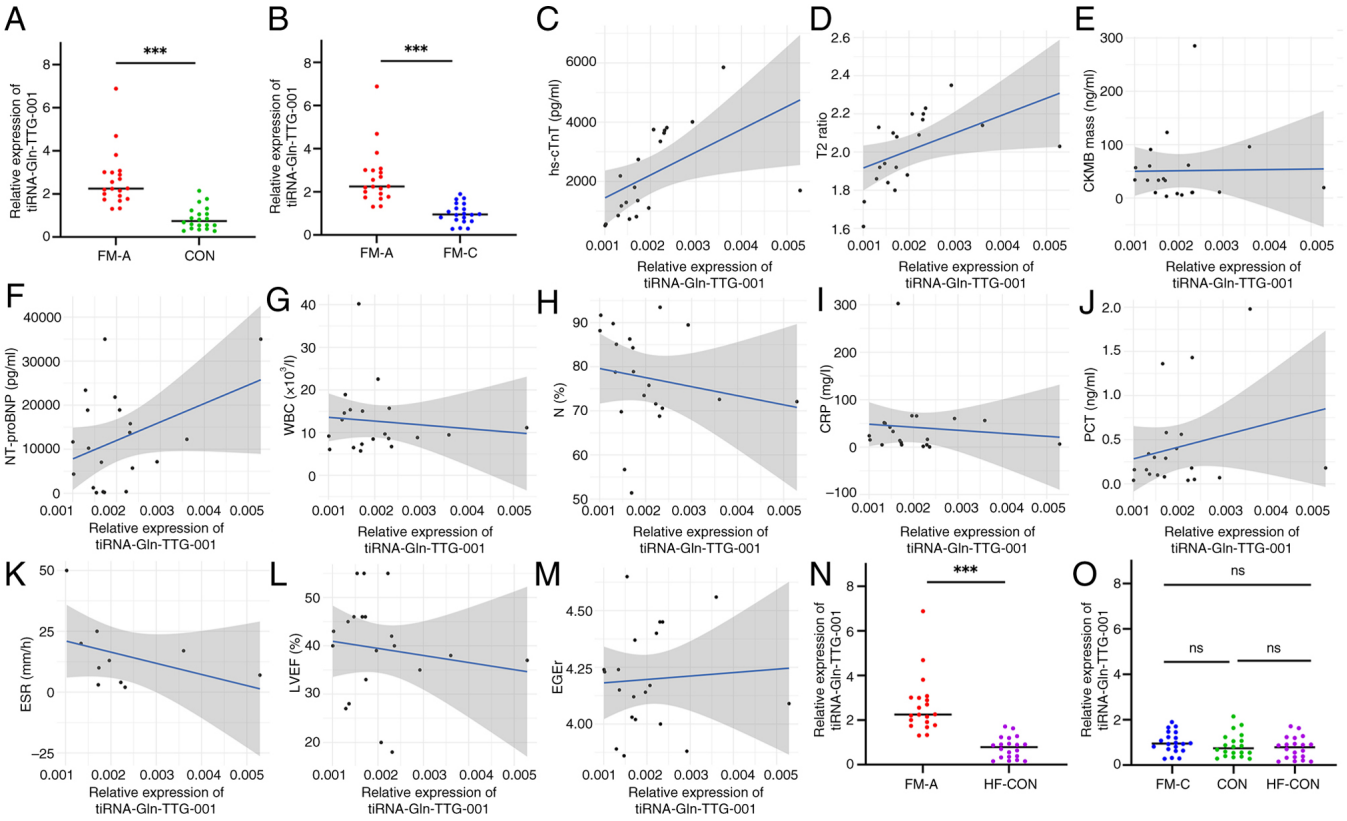

Figure 1. Clinical significance of 5'tiRNA-Gln-TTG-001. Expression levels of 5'tiRNA-Gln-TTG-001 in (A) FM-A and CON, and in (B) FM-A and FM-C were detected by RT-qPCR. Expression levels of 5'tiRNA-Gln-TTG-001 demonstrated a positive correlation with (C) hs-cTnT values and (D) the T2 ratio. No significance was observed between the relative expression levels of 5'tiRNA-Gln-TTG-001 and (E) CKMB mass, (F) NT-proBNP, (G) WBC, (H) N%, (I) CRP, (J) PCT, (K) ESR, (L) LVEF and (M) EGEr. Expression levels of 5'tiRNA-Gln-TTG-001 in (N) FM-A and HF-CON, and in (O) FM-C, FM-A and HF-CON were detected by RT-qPCR, and no significant differences were observed among FM-C, CON and HF-CON. Data are presented as the mean ± SD. ***P<0.001; ns, not significant (P>0.05). CKMB, creatine kinase MB; CON, control; CRP, C-reactive protein; EGEr, early gadolinium enhancement ratio; ESR, erythrocyte sedimentation rate; FM, fulminant myocarditis; FM-A, acute FM; FM-C, convalescent FM; hs-cTnT, high-sensitivity cardiac troponin; LVEF, left ventricular ejection fraction; N, neutrophil ratio; NT-proBNP, N-terminal pro-B-type natriuretic peptide; PCT, procalcitonin; RT-qPCR, reverse transcription-quantitative PCR; tiRNA, transfer RNA-derived stress-induced RNA; WBC, white blood cell count.

(DAPI) stained the nucleus. No red or green fluorescence signal was detected in the NC, suggesting the dual nuclear and cytoplasmic localization of 5'tiRNA-Gln-TTG-001 in cardiomyocytes.

Dynamic expression of 5'tiRNA-Gln-TTG-001 in a cardiomyocyte inflammatory injury model. Upregulation of plasma 5'tiRNA-Gln-TTG-001 in acute myocarditis and its expression in AC16 cells prompted the exploration of its potential involvement in cardiomyocyte inflammatory injury. Due to the absence of the homologous sequence for human 5'tiRNA-Gln-TTG-001 in mice, rats or rabbits, the present study focused on an *in vitro* cardiomyocyte system modeling inflammatory injury. To validate the feasibility of an *in vitro* model mimicking myocarditis by exposing AC16 to LPS, expression levels of TLR4, the receptor of LPS that drives the inflammatory response, and its associated factors, including LY96 and subunits of NF-κB, such as RelA and NF-κB1, were assessed. Analysis revealed the expression of TLR4 and its associated factors in AC16 cells (Fig. 3A). To verify the successful establishment of the cardiomyocyte inflammatory injury model, cell viability, apoptosis rates, inflammatory markers (IL-1β, IL-6 and IL-18), myocardial injury markers (CKMB and cTnT) and a myocardial dysfunction marker (NT-proBNP) were evaluated. Analysis revealed the establishment of the *in vitro* model characterized by decreased cell viability (Fig. 3B), increased apoptosis rates (Fig. 3C and D), along with increased inflammatory markers, including IL-1β and IL-18 at both the transcript and protein levels, and IL-6 at the protein level (Fig. 3E and F), and myocardial injury biomarkers (CKMB and cTnT; Fig. 3G). No significant differences were observed in the concentration of NT-proBNP (Fig. 3G). After assessing the feasibility and quantification of the *in vitro* model, the dynamic expression of 5'tiRNA-Gln-TTG-001 was analyzed in AC16 cells at 0, 12, 24, 36 and 48 h following LPS stimulation. Analysis revealed that 5'tiRNA-Gln-TTG-001 expression levels were increased with prolonged stimulation time, with the exception of at 12 h (Fig. 3H).

Cardiomyocyte inflammatory injury is aggravated by 5'tiRNA-Gln-TTG-001. Given the significant upregulation of 5'tiRNA-Gln-TTG-001 in the cardiomyocyte inflammatory injury model, it was hypothesized that it could have a potential role in aggravating myocarditis. Accordingly, gain-of-function and loss-of-function experiments were carried out to assess the biological function of 5'tiRNA-Gln-TTG-001. tiRNA mimics and inhibitors were used to upregulate and downregulate 5'tiRNA-Gln-TTG-001

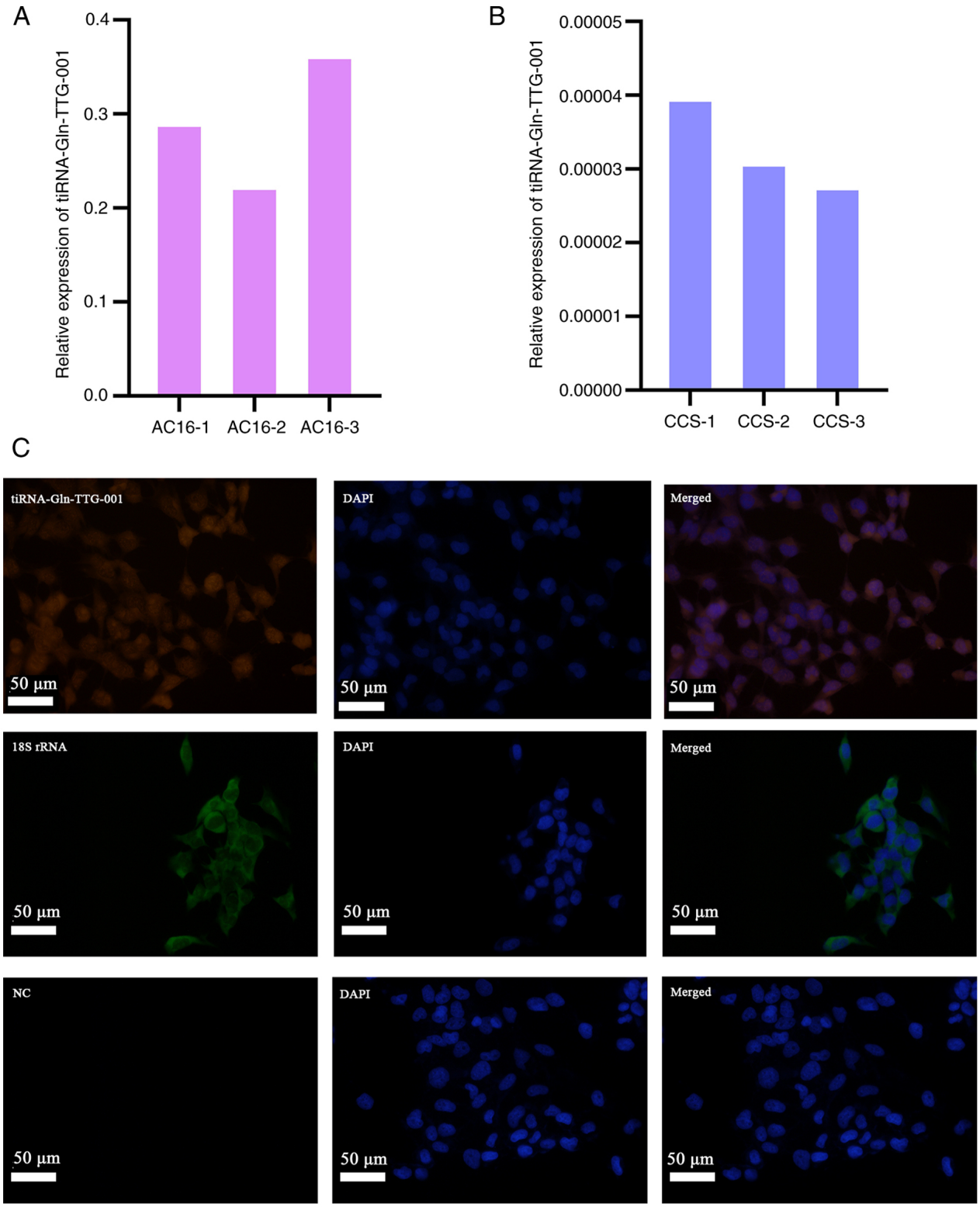

Figure 2. Origin and subcellular localization of 5'tiRNA-Gln-TTG-001. (A) Expression levels of 5'tiRNA-Gln-TTG-001 from AC16 cells were detected by RT-qPCR. Representative data from three discrete experiments (AC16-1, AC16-2 and AC16-3) are shown. These data are presented as visual representations only and have not been analyzed statistically. (B) Expression levels of 5'tiRNA-Gln-TTG-001 from CCS were detected by RT-qPCR. Data from three distinct experiments (CCS-1, CCS-2 and CCS-3) are presented. These data are displayed solely as visual representations and have not undergone statistical analysis. (C) RNA-FISH demonstrated distribution of 5'tiRNA-Gln-TTG-001 within both the cytoplasmic and nuclear compartments, 18S rRNA (labelled with carboxyfluorescein, green) exclusively in the cytoplasm, and the absence of signal in the NC. 5'tiRNA-Gln-TTG-001 probes were labeled with cyanine 3 (red). Nuclei were stained with DAPI (blue). Scale bar, 50 μm. All experiments were independently replicated at least three times. CCS, cell culture supernatant; FISH, fluorescence *in situ* hybridization; NC, negative control; tiRNA, transfer RNA-derived stress-induced RNA.

expression levels, respectively, with transfection efficiency validated by RT-qPCR assays (Fig. 4A). CCK-8 assays demonstrated that overexpressing 5'tiRNA-Gln-TTG-001 reduced cell viability both in the absence of LPS when

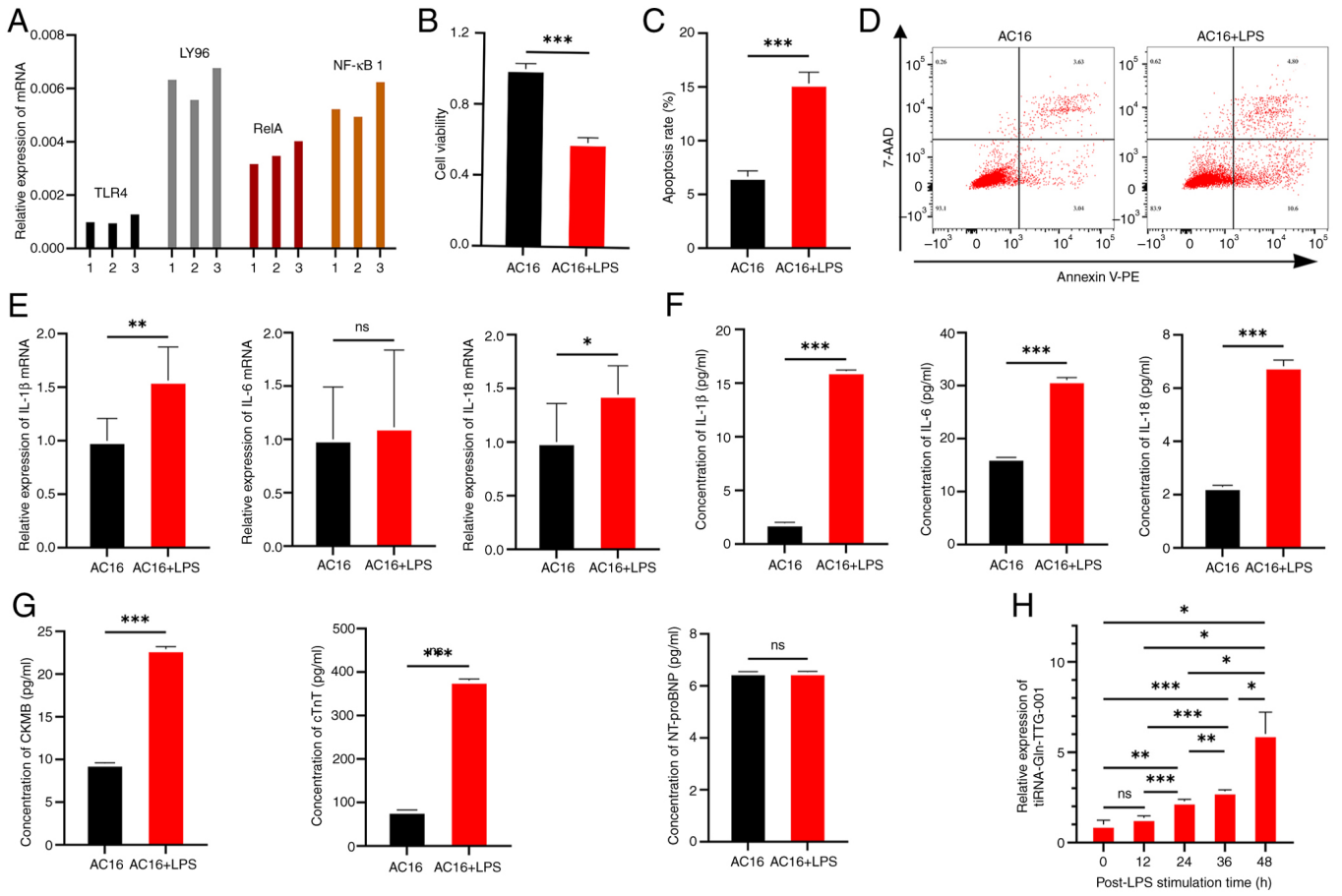

Figure 3. Establishment of the cell model mimicking myocarditis and dynamic expression of 5'tiRNA-Gln-TTG-001. (A) Expression levels of TLR4, LY96, RelA and NF-kB1. Representative data from three distinct experiments are presented. These data are provided solely as visual representations and have not undergone statistical analysis. (B) Cell viability was measured using the Cell Counting Kit-8 assay with or without LPS stimulation. Apoptosis was assessed utilizing an Annexin V-PE/7-AAD double staining protocol in conjunction with a flow cytometry-based apoptosis assay with or without LPS stimulation; (C) quantification of results and (D) representative images. (E) Expression levels of IL-1β, IL-6 and IL-18 were detected by RT-qPCR with or without LPS stimulation. (F) Levels of IL-1β, IL-6 and IL-18 were detected by ELISA with or without LPS stimulation. (G) Levels of CKMB, cTnT and NT-proBNP were detected by ELISA with or without LPS stimulation. (H) Expression levels of 5'tiRNA-Gln-TTG-001 secreted from AC16 cells were detected by RT-qPCR at 0, 12, 24, 36 and 48 h post-LPS stimulation, and they were markedly elevated at 48, 36 and 24 h compared with all earlier time points but did not differ at 12 h compared with at 0 h. Data are presented as the mean ± SD. *P<0.05, **P<0.01, ***P<0.001; ns, not significant (P>0.05). 7-AAD, 7-aminoactinomycin D; CKMB, creatine kinase MB; cTnT, cardiac troponin; LPS, lipopolysaccharide; LY96, lymphocyte antigen 96; NT-proBNP, N-terminal pro-B-type natriuretic peptide; PE, phycoerythrin; RT-qPCR, reverse transcription-quantitative PCR; tiRNA, transfer RNA-derived stress-induced RNA; TLR4, Toll-like receptor 4.

compared with AC16 cells and in the presence of LPS when compared with AC16 + LPS cells; whereas knockdown of 5'tiRNA-Gln-TTG-001 in LPS-treated samples increased cell viability when compared with AC16 + LPS samples (Fig. 4B). The impact of 5'tiRNA-Gln-TTG-001 overexpression and inhibition was subsequently examined in AC16 cell apoptosis using flow cytometry. As shown in Fig. 4C and D, increased apoptosis rates were observed upon overexpression of 5'tiRNA-Gln-TTG-001. As expected, knockdown of 5'tiRNA-Gln-TTG-001 expression significantly decreased the apoptosis rates of AC16 cells. Finally, RT-qPCR and ELISA revealed that increased levels of 5'tiRNA-Gln-TTG-001 upregulated inflammatory markers, including both transcript and protein levels of IL-1β, IL-6 and IL-18 (Fig. 4E and F), and myocardial injury biomarkers, including CKMB and cTnT protein levels (Fig. 4G), when exposed to LPS. By contrast, knockdown of 5'tiRNA-Gln-TTG-001 reduced the transcript and protein levels of inflammatory markers IL-1β and IL-18, and protein levels of IL-6 (Fig. 4E and F), and the protein levels of myocardial injury biomarkers, including CKMB and cTnT (Fig. 4G), when exposed to LPS. No significant differences were observed in NT-proBNP protein levels (Fig. 4G). Overall, these findings suggested that overexpressing 5'tiRNA-Gln-TTG-001 may decrease viability, and aggravate apoptosis, inflammation and myocardial injury in AC16 cells, whereas its inhibition exhibited contrasting effects under LPS exposure.

CLIC4 is upregulated by direct binding of 5'tiRNA-Gln-TTG-001. The findings of the present study indicated that overexpressing 5'tiRNA-Gln-TTG-001 may yield proinflammatory effects in AC16 cells. To gain mechanistic insights, the underlying mechanism by which 5'tiRNA-Gln-TTG-001 regulates myocarditis progression was investigated. Given the established role of tiRNAs in disease through direct interaction with target genes (29-34), it was hypothesized that 5'tiRNA-Gln-TTG-001 might contribute to pathogenesis by binding to target genes. To verify CLIC4 as the target gene of 5'tiRNA-Gln-TTG-001, the temporal, spatial and structural relationships between

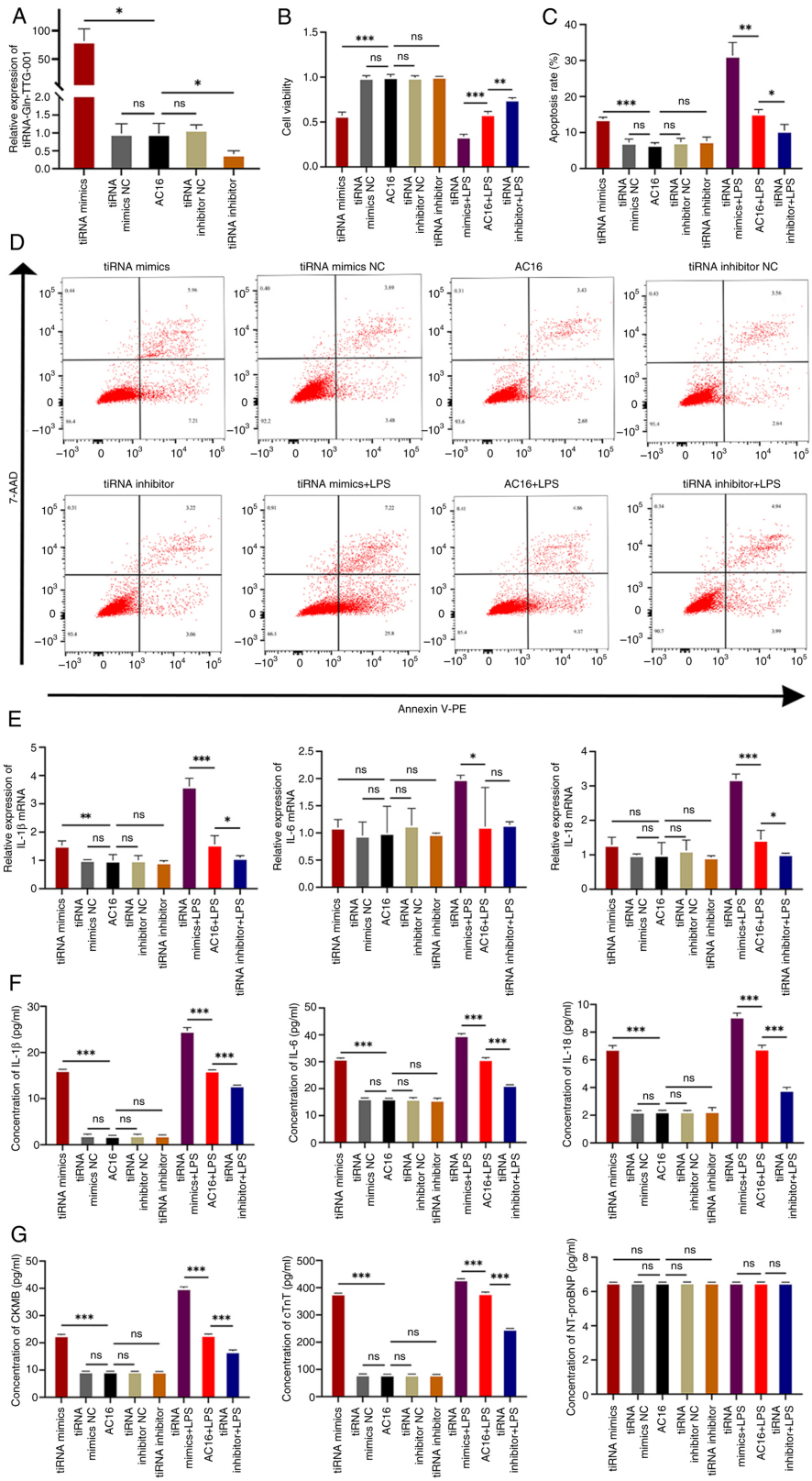

Figure 4. Pathophysiological functions of 5'tiRNA-Gln-TTG-001 in cardiomyocyte inflammatory injury. (A) Efficiency of overexpression or knockdown of 5'tiRNA-Gln-TTG-001 in AC16 was detected by RT-qPCR. (B) Cell viability was measured using the Cell Counting Kit-8 when transiently transfected with 5'tiRNA-Gln-TTG-001 mimics or inhibitors with or without LPS stimulation. Apoptosis was assessed utilizing an Annexin V-PE/7-AAD double staining protocol in conjunction with a flow cytometry-based apoptosis assay when transiently transfected with 5'tiRNA-Gln-TTG-001 mimics or inhibitors with or without LPS stimulation; (C) quantification of results and (D) representative images. (E) Expression levels of IL-1β, IL-6 and IL-18 were detected by RT-qPCR when transiently transfected with 5'tiRNA-Gln-TTG-001 mimics or inhibitors with or without LPS stimulation. (F) Levels of IL-1β, IL-6 and IL-18 were detected by ELISA when transiently transfected with 5'tiRNA-Gln-TTG-001 mimics or inhibitors with or without LPS stimulation. (G) Levels of CKMB, cTnT and NT-proBNP were detected by ELISA when transiently transfected with 5'tiRNA-Gln-TTG-001 mimics or inhibitors with or without LPS stimulation. Data are presented as the mean ± SD. *P<0.05, **P<0.01, ***P<0.001; ns, not significant (P>0.05). 7-AAD, 7-aminoactinomycin D; CKMB, creatine kinase MB; cTnT, cardiac troponin T; LPS, lipopolysaccharide; NC, negative control; NT-proBNP, N-terminal pro-B-type natriuretic peptide; PE, phycoerythrin; RT-qPCR, reverse transcription-quantitative PCR; tiRNA, transfer RNA-derived stress-induced RNA.

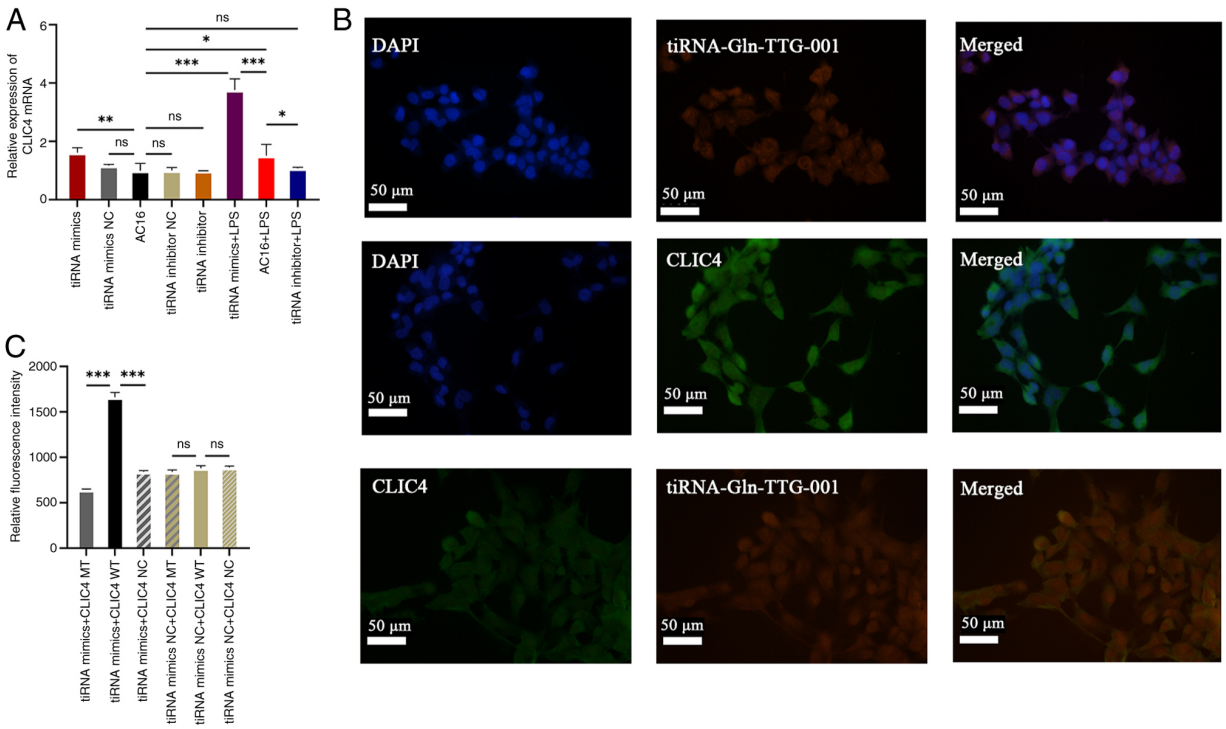

Figure 5. Temporal, spatial and structural association between 5'tiRNA-Gln-TTG-001 and CLIC4. (A) Expression levels of CLIC4 in AC16 cells transiently transfected with 5'tiRNA-Gln-TTG-001 mimics or inhibitors with or without LPS stimulation were detected by reverse transcription-quantitative PCR. (B) RNA-fluorescence *in situ* hybridization revealed the cytosolic colocalization of 5'tiRNA-Gln-TTG-001 and CLIC4 in AC16 human cardiomyocytes. Probes for 5'tiRNA-Gln-TTG-001 were labeled with cyanine 3 (red). CLIC4 probes were labeled with carboxyfluorescein (green). Nuclei were stained with DAPI (blue). Scale bar, 50 μm. (C) Luciferase reporter assay verified the molecular interactions between 5'tiRNA-Gln-TTG-001 and the 3'untranslated region of CLIC4 WT transcripts. Data are presented as the mean ± SD. *P<0.05; **P<0.01; ***P<0.001; ns, not significant (P>0.05). CLIC4, chloride intracellular channel 4; LPS, lipopolysaccharide; MT, mutant; NC, negative control; tiRNA, transfer RNA-derived stress-induced RNA; WT, wild-type.

5'tiRNA-Gln-TTG-001 and CLIC4 were examined. Initially, the regulatory effect of 5'tiRNA-Gln-TTG-001 on CLIC4 mRNA expression was investigated. Analysis revealed that upregulation of 5'tiRNA-Gln-TTG-001 in AC16 cells significantly induced CLIC4 mRNA expression irrespective of LPS exposure (Fig. 5A), whereas silencing 5'tiRNA-Gln-TTG-001 reduced CLIC4 mRNA expression in AC16 cells treated with LPS (Fig. 5A). Similarly, Jehn *et al* (34) revealed that certain 5'tiRNAs could sequence-specifically upregulate mRNAs. Subsequently, the cellular localization of 5'tiRNA-Gln-TTG-001 and CLIC4 was examined by RNA-FISH analysis, which revealed co-localization of 5'tiRNA-Gln-TTG-001 (red fluorescence) and CLIC4 mRNA (green fluorescence) in both cytoplasmic and nuclear compartments (Fig. 5B). To further validate the 5'tiRNA-Gln-TTG-001 binding sites on the target mRNAs, dual-luciferase reporter assays were adopted. CLIC4 WT, CLIC4 MT and CLIC4 NC 3'UTRs were synthesized and subsequently cloned into the luciferase reporter vector (Fig. 5C). In comparison with CLIC4 NC or CLIC4 MT, the 5'tiRNA-Gln-TTG-001 mimics markedly increased the activity of the CLIC4 WT-fused luciferase reporter (Fig. 5C). These findings collectively indicated that 5'tiRNA-Gln-TTG-001 may directly interact with specific sites on CLIC4 mRNA, influencing its expression.

Cardiomyocyte inflammatory injury is aggravated by 5'tiRNA-Gln-TTG-001 via CLIC4. Upon establishment that 5'tiRNA-Gln-TTG-001 could modulate cardiomyocyte inflammatory injury and regulate CLIC4 mRNA expression in AC16 cells, and considering CLIC4 has been revealed as a key regulator of apoptosis (22-24) and a key mediator of inflammation (25), it was hypothesized that 5'tiRNA-Gln-TTG-001 may exert proinflammatory effects in acute myocarditis by regulating CLIC4 expression. Rescue experiments were conducted to confirm this hypothesis. AC16 cells were co-transfected with 5'tiRNA-Gln-TTG-001 mimics and CLIC4 siRNA, and compared with cells transfected with 5'tiRNA-Gln-TTG-001 mimics alone. Furthermore, AC16 cells were co-transfected with 5'tiRNA-Gln-TTG-001 inhibitors and a CLIC4 overexpression plasmid, and compared with cells transfected with 5'tiRNA-Gln-TTG-001 inhibitors alone. The overexpression and knockdown efficiencies of CLIC4 are shown in Fig. 6A. RT-qPCR revealed that the CLIC4 overexpression plasmid and CLIC4 siRNA could upregulate and downregulate the expression levels of CLIC4, respectively (Fig. 6B). The CCK-8 assays indicated a significant reduction in AC16 cell viability following the overexpression of 5'tiRNA-Gln-TTG-001 via tiRNA mimics, which was reversed by CLIC4 knockdown (Fig. 6C). Flow cytometric analysis indicated that the upregulation of 5'tiRNA-Gln-TTG-001 increased cell apoptosis rates, an effect significantly mitigated by CLIC4 siRNA (Fig. 6D). Overexpression of 5'tiRNA-Gln-TTG-001 significantly increased inflammatory markers (IL-1β, IL-6 and IL-18) and myocardial injury markers (CKMB and cTnT), which could be rescued by CLIC4 knockdown (Fig. 6E-G).

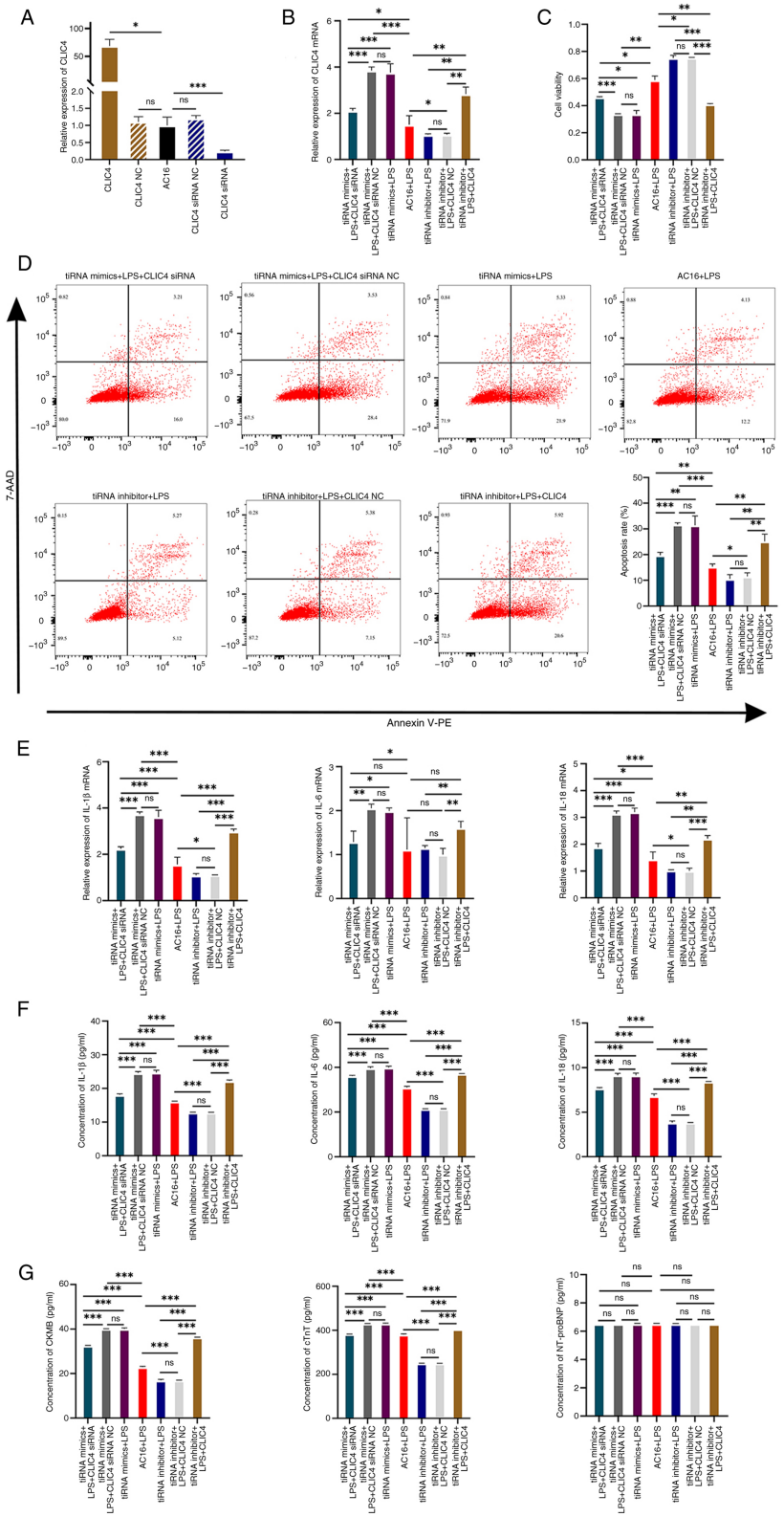

Figure 6. Downregulation of CLIC4 reverses the effects of upregulation of 5'tiRNA-Gln-TTG-001 on cardiomyocyte inflammatory injury. (A) Efficiency of overexpression or knockdown of CLIC4 in AC16 human cardiomyocytes was detected by RT-qPCR. (B) Expression levels of CLIC4 in transfected AC16 were detected by RT-qPCR. (C) Cell viability was measured using the Cell Counting Kit-8 when transiently co-transfected with tiRNA mimics and CLIC4 siRNA or tiRNA inhibitor and the CLIC4 overexpression plasmid with LPS stimulation. (D) Apoptosis was detected with Annexin V-PE/7-AAD double staining using a flow cytometry apoptosis assay. (E) Expression levels of IL-1β, IL-6 and IL-18 were detected by RT-qPCR when co-transfected with tiRNA mimics and CLIC4 siRNA or tiRNA inhibitor and the CLIC4 overexpression plasmid with LPS stimulation. (F) Levels of IL-1β, IL-6 and IL-18 were detected by ELISA when co-transfected with tiRNA mimics and CLIC4 siRNA or tiRNA inhibitor and the CLIC4 overexpression plasmid with LPS stimulation. (G) Levels of CKMB, cTnT, and NT-proBNP were detected by ELISA when co-transfected with tiRNA mimics and CLIC4 siRNA or tiRNA inhibitor and the CLIC4 overexpression plasmid with LPS stimulation. Data are presented as the mean ± SD. *P<0.05, **P<0.01, ***P<0.001; ns, not significant (P>0.05). 7-AAD, 7-aminoactinomycin D; CKMB, creatine kinase MB; CLIC4, chloride intracellular channel 4; cTnT, cardiac troponin T; LPS, lipopolysaccharide; NC, negative control; NT-proBNP, N-terminal pro-B-type natriuretic peptide; PE, phycoerythrin; RT-qPCR, reverse transcription-quantitative PCR; siRNA, small interfering RNA; tiRNA, transfer RNA-derived stress-induced RNA.

Consistently, tiRNA inhibitor-mediated knockdown of 5'tiRNA-Gln-TTG-001 yielded a significant increase in cell viability (Fig. 6C) and a significant reduction in apoptosis (Fig. 6D), and levels of pro-inflammatory cytokines (IL-1β and IL-18 transcript and protein levels, in addition to IL-6 protein levels) and myocardial injury biomarkers (cTnT and CKMB protein levels; Fig. 6E-G), which could be prevented by overexpression of CLIC4. No significant differences were observed in NT-proBNP (Fig. 6G). Overall, these findings suggested that 5'tiRNA-Gln-TTG-001 aggravated cardiomyocyte inflammatory injury through upregulation of CLIC4.

Discussion

Acute myocarditis refers to a group of cardiac inflammatory diseases characterized by ongoing active cardiomyocyte inflammatory injury and can be classified into subclinical, clinical and FM based on clinical features (4). FM is a type of acute myocarditis characterized by rapid hemodynamic collapse and a potentially fatal outcome (4). The disease typically progresses through a 1-2-week acute phase, followed by a recovery phase. Current understanding of the pathophysiology of myocarditis is mainly derived from experimental murine studies of cardiotropic viruses and remains poorly elucidated (3-6). tsRNAs represent a distinct subclass of small non-coding RNAs and carry out diverse roles in physiological and pathological processes, potentially offering opportunities for improved diagnosis and novel therapeutic strategies (14-18). However, the understanding of tsRNA expression and functions in the heart and cardiovascular diseases remains limited. In our previous study (20), differential plasma tsRNA expression profiles were obtained from juveniles with FM and a novel tsRNA, 5'tiRNA-Gln-TTG-001 was identified, which exhibited upregulated expression in the acute phase of myocarditis. These findings suggest that 5'tiRNA-Gln-TTG-001 contributes to the inflammatory progression of myocarditis.

The present study expanded the sample size to examine the clinical significance of 5'tiRNA-Gln-TTG-001, revealing that its plasma levels significantly increased during the acute phase of myocarditis and subsequently decreased during the convalescent phase, indicating its role in the initiation and progression of the condition. The selection of juveniles clinically diagnosed with FM as research subjects was based on the fact that FM is a clinical diagnosis that generates considerably less diagnostic controversy compared with non-FM acute myocarditis (35). Furthermore, to minimize errors due to clinical misdiagnosis of myocarditis, strict inclusion and exclusion criteria were adhered to. Moreover, the association between 5'tiRNA-Gln-TTG-001 expression levels and conventional clinical indices recommended for screening in the diagnosis of myocarditis by current guidelines was analyzed (3-6,9). The present study observed that 5'tiRNA-Gln-TTG-001 expression levels exhibited a correlation with hs-cTnT (a myocardial injury marker) and T2 ratio (reflecting myocardial edema). These findings suggest that 5'tiRNA-Gln-TTG-001 could serve as a diagnostic biomarker for acute myocarditis.

To assess specificity, 5'tiRNA-Gln-TTG-001 expression was evaluated in patients with myocarditis against those with DCM and chronic heart failure during acute decompensation episodes, a condition often difficult to distinguish from acute myocarditis. The findings revealed significantly increased 5'tiRNA-Gln-TTG-001 levels in acute myocarditis, indicating its potential specificity for this condition, offering a novel approach for distinguishing acute myocarditis from chronic heart failure during acute decompensation episodes. These findings collectively support 5'tiRNA-Gln-TTG-001 as a promising diagnostic tool. Due to the rarity of FM cases in juveniles, and the strict inclusion and exclusion criteria, the number of study subjects was relatively small. While the present study suggests the potential of 5'tiRNA-Gln-TTG-001 as a biomarker for acute myocarditis, additional validation through larger, multicenter studies is required. In addition, the precise stressors that trigger tRNA cleavage and the origins of these circulating tsRNAs in the present study remain unidentified. tiRNAs are generated through the specific cleavage of mature tRNA under cellular stress (36). It has long been considered that tiRNAs were formed by angiogenin-mediated cleavage of mature tRNA under stress conditions; however, in 2019, Su *et al* (37) revealed that knockout of angiogenin did not affect the generation of the majority of tiRNAs, while overexpression of angiogenin only selectively degraded a subset of tiRNAs. This indicates that tiRNA biogenesis is not entirely dependent on angiogenin and suggests the existence of other unknown generation mechanisms. Given that tRNA cleavage has been observed in association with various physiological and pathological processes (16,36,38,39), it is highly conceivable that these mechanisms may carry out a role in the tRNA cleavage observed in the present study.

In light of the lack of a homologous sequence for human 5'tiRNA-Gln-TTG-001 in rodent models, and its presence in both the nucleus and cytoplasm of cardiomyocytes, an *in vitro* and inflammatory injury model was employed in cardiomyocytes, simulating myocarditis by treating AC16 cells with LPS, to explore the pathobiological effects and mechanisms of 5'tiRNA-Gln-TTG-001. The selection of LPS-induced inflammation was based on the following two points: i) LPS is a bacterial-derived molecule that activates TLR4, leading to the promotion of angiogenin, which cleaves tRNAs within anticodon loops to produce tiRNAs (40). ii) LPS can induce the expression of CLIC4, a predicted target of 5'tiRNA-Gln-TTG-001, to produce inflammatory cytokines (25). After validating the feasibility and quantification of the cardiomyocyte inflammatory injury model, the present study verified that 5'tiRNA-Gln-TTG-001 production increased with LPS stimulation, demonstrating increased levels with prolonged exposure. This finding aligned with observations in the acute phase of myocarditis in the present study. Furthermore, subsequent *in vitro* gain-of-function and loss-of-function experiments demonstrated that 5'tiRNA-Gln-TTG-001 reduced cell viability, increased apoptosis, and aggravated both myocardial inflammation and injury. The proinflammatory effects of 5'tiRNA-Gln-TTG-001 in myocarditis highlight its potential as a therapeutic target for acute myocarditis treatment.

Based on the aforementioned findings, the present study further sought to elucidate the molecular mechanisms by which 5'tiRNA-Gln-TTG-001 promotes myocarditis. Given that tsRNAs share similarities in length and effects with

miRNAs suggests that the mechanism involves direct binding to the 3'UTR of downstream targets analogous to the canonical miRNA pathway. For example, Zong *et al* (33) revealed that 5'-tiRNA-Cys-GCA could bind to the 3'UTR of STAT4 to modulate vascular smooth muscle cell proliferation and phenotypic transition in aortic dissection. Bioinformatics analysis identified CLIC4 as a potential direct downstream target of 5'tiRNA-Gln-TTG-001, which was subsequently validated through experiments. RNA-FISH analysis demonstrated the co-localization of 5'tiRNA-Gln-TTG-001 and CLIC4 in both the nucleus and cytoplasm. Gain-of-function and loss-of-function experiments demonstrated that 5'tiRNA-Gln-TTG-001 enhanced CLIC4 expression. Finally, dual-luciferase reporter assays indicated that 5'tiRNA-Gln-TTG-001 activated CLIC4 by binding to its 3'UTR.

Overall, the findings of the present study indicate that 5'tiRNA-Gln-TTG-001 may act as an upstream regulator of CLIC4 expression levels, a mechanism identified for the first time in the present study, to the best of our knowledge. Similarly, Jehn *et al* (34) revealed that certain 5'tiRNAs can sequence-specifically upregulate mRNAs, suggesting non-miRNA-like targeting rules. To elucidate this phenomenon, they used a novel k-mer mapping methodology and suggested the existence of an as-yet-unknown regulatory mechanism that certain 5'tiRNAs can stabilize mRNAs in a sequence-specific manner (34). Furthermore, it is important to acknowledge that in addition to the miRNA-like pathway, the molecular mechanisms of tsRNAs also encompass the following: i) P-element-induced wimpy testis (PIWI) protein complex formation, involving interactions with PIWI proteins to facilitate targeted DNA methylation (41); ii) RNA-binding protein interactions, where tsRNAs regulate protein translation through associations with RNA-binding proteins such as Y-box binding protein 1 and reverse transcriptase (42); iii) intergenerational inheritance, whereby specific tsRNAs are imported into sperm via epididymal epithelial cells, thereby affecting transgenerational epigenetic inheritance (43); iv) mRNA stability modulation, through direct or indirect effects on mRNA stability (44); v) non-coding RNA stability regulation, impacting the stability of other non-coding RNAs (45); vi) ribosome interaction, where tsRNAs enhance or interfere with ribosome assembly and function to regulate protein translation (38).

Having confirmed that CLIC4 was a target gene of 5'tiRNA-Gln-TTG-001, the present study ultimately identified 5'tiRNA-Gln-TTG-001 as a proinflammatory modulator of cardiomyocytes through the upregulation of CLIC4, as confirmed by rescue assays. CLIC4 is predominantly found in the heart, kidneys and skeletal muscles (21), where it regulates apoptosis. It is upregulated by DNA damage and contributes to the p53-mediated apoptotic response (22). Overexpression of CLIC4 has been demonstrated to induce the activation of caspase (23). It is also a key regulator of inflammation, and macrophage lines overexpressing CLIC4 produce more inflammatory cytokines when exposed to LPS (25). Malik *et al* (46) revealed that nuclear translocation of CLIC4 is a key element in the macrophage deactivation process. Consequently, the present study proposes targeting the 5'tiRNA-Gln-TTG-001/CLIC4 axis as a potential therapeutic strategy for myocarditis. However, the possibility of additional key gene targets of 5'tiRNA-Gln-TTG-001 beyond CLIC4 or other mechanisms that may considerably contribute to the progression of myocarditis cannot be ruled out.

Several limitations in the present study should be acknowledged. First, the study participants did not undergo EMB, hindering the ability to establish a definitive correlation between plasma and myocardial expression of 5'tiRNA-Gln-TTG-001. Second, the relatively small sample size due to strict inclusion and exclusion criteria of the present study necessitates further validation in larger cohorts. Third, the chemically synthesized 5'tiRNA-Gln-TTG-001 mimics may not fully replicate modification-dependent functions, potentially affecting their biological relevance. Fourth, the immortalized human cardiomyocyte cell lines employed in the present study were incapable of generating action potentials.

In future research, it would be beneficial to employ customized humanized mouse models for *in vivo* experimental validation to substantiate the function of the findings of the present study and to investigate further the underlying mechanisms by which 5'tiRNA-Gln-TTG-001 modulates cardiomyocyte inflammatory injury through CLIC4. Furthermore, the use of cardiac organoids could offer a complementary method for conducting detailed functional studies.

In summary, to the best of our knowledge, the present study provides the first evidence that 5'tiRNA-Gln-TTG-001 is significantly upregulated in acute myocarditis and markedly aggravates myocardial inflammatory injury. The underlying mechanism involves its sequence-specific upregulation of CLIC4. The findings demonstrate that 5'tiRNA-Gln-TTG-001 could potentially serve as a promising novel biomarker for the diagnosis of myocarditis, enabling differentiation from DCM with decompensated heart failure. Furthermore, these results shed new light on the tsRNAs-mediated pathophysiological mechanisms involved in myocarditis, offering a potential therapeutic target to expand treatment options.

Acknowledgements

Not applicable.

Funding

This work was supported by grants from the Natural Science Foundation of Shandong Province, China (grant no. ZR2023MH181) and the National Natural Science Foundation of China (grant no. 81873498).

Availability of data and materials

The data generated in the present study may be requested from the corresponding author.

Authors' contributions

JW and BH contributed to the conception and design of the present study. JW, YY and LZ carried out the principal experiments. JW, YY and HJ contributed to the analysis and interpretation of the data. JW and YY contributed to the writing of the original draft. All authors contributed to the review and editing of the final draft. JW, BH and LZ confirm

the authenticity of all the raw data. All authors read and approved the final manuscript.

Ethics approval and consent to participate

This study was approved by the ethics committee of Shandong Provincial Hospital, Jinan, China (approval no. 2018-115) and was carried out in accordance with The Declaration of Helsinki. Written informed consent has been obtained from the parents of each pediatric patient (<18 years old).

Patient consent for publication

Not applicable.

Competing interests

The authors declare that that they have no competing interests.

References

1. Ammirati E and Moslehi JJ: Diagnosis and treatment of acute myocarditis: A review. JAMA 329: 1098-1113, 2023.
2. Basso C and Longo DL: Myocarditis. N Engl J Med 387: 1488-1500, 2022.
3. Caforio ALP, Pankuweit S, Arbustini E, Basso C, Gimeno-Blanes J, Felix SB, Fu M, Heliö T, Heymans S, Jahns R, *et al*: Current state of knowledge on aetiology, diagnosis, management, and therapy of myocarditis: A position statement of the European society of cardiology working group on myocardial and pericardial diseases. Eur Heart J 34: 2636-2648, 2013.
4. Nagai T, Inomata T, Kohno T, Sato T, Tada A, Kubo T, Nakamura K, Oyama-Manabe N, Ikeda Y, Fujino T, *et al*: JCS 2023 guideline on the diagnosis and treatment of myocarditis. Circ J 87: 674-754, 2023.
5. Friedrich MG, Sechtem U, Schulz-Menger J, Holmvang G, Alakija P, Cooper LT, White JA, Abdel-Aty H, Gutberlet M, Prasad S, *et al*: Cardiovascular magnetic resonance in myocarditis: A JACC white paper. J Am Coll Cardiol 53: 1475-1487, 2009.
6. Ferreira VM, Schulz-Menger J, Holmvang G, Kramer CM, Carbone I, Sechtem U, Kindermann I, Gutberlet M, Cooper LT, Liu P and Friedrich MG: Cardiovascular magnetic resonance in nonischemic myocardial inflammation: Expert recommendations. J Am Coll Cardiol 72: 3158-3176, 2018.
7. Law YM, Lal AK, Chen S, Čiháková D, Cooper LT Jr, Deshpande S, Godown J, Grosse-Wortmann L, Robinson JD and Towbin JA; American Heart Association Pediatric Heart Failure and Transplantation Committee of the Council on Lifelong Congenital Heart Disease and Heart Health in the Young and Stroke Council: Diagnosis and management of myocarditis in children: A scientific statement from the American heart association. Circulation 144: e123-e135, 2021.
8. Bernhard B, Marxer ME, Zurkirchen JC, Schütze J, Wahl A, Elchinova E, Spano G, Boscolo Berto M, Wieser M, Garefa C, *et al*: Prognostic implications of clinical and imaging diagnostic criteria for myocarditis. J Am Coll Cardiol 84: 1373-1387, 2024.
9. Kociol RD, Cooper LT, Fang JC, Moslehi JJ, Pang PS, Sabe MA, Shah RV, Sims DB, Thiene G and Vardeny O; American Heart Association Heart Failure and Transplantation Committee of the Council on Clinical Cardiology: Recognition and initial management of fulminant myocarditis: A scientific statement from the American heart association. Circulation 141: e69-e92, 2020.
10. Caforio ALP, Kaski JP, Gimeno JR, Elliott PM, Laroche C, Tavazzi L, Tendera M, Fu M, Sala S, Seferovic PM, *et al*: Endomyocardial biopsy: Safety and prognostic utility in paediatric and adult myocarditis in the European Society of cardiology EURObservational research programme cardiomyopathy and myocarditis long-term registry. Eur Heart J 45: 2548-2569, 2024.
11. Lee YS, Shibata Y, Malhotra A and Dutta A: A novel class of small RNAs: tRNA-derived RNA fragments (tRFs). Genes Dev 23: 2639-2649, 2009.
12. Schimmel P: The emerging complexity of the tRNA world: Mammalian tRNAs beyond protein synthesis. Nat Rev Mol Cell Biol 19: 45-58, 2018.
13. Magee R and Rigoutsos I: On the expanding roles of tRNA fragments in modulating cell behavior. Nucleic Acids Res 48: 9433-9448, 2020.
14. Ruggero K, Guffanti A, Corradin A, Sharma VK, De Bellis G, Corti G, Grassi A, Zanovello P, Bronte V, Ciminale V and D'Agostino DM: Small noncoding RNAs in cells transformed by human T-cell leukemia virus type 1: A role for a tRNA fragment as a primer for reverse transcriptase. J Virol 88: 3612-3622, 2014.
15. Geng G, Wang H, Xin W, Liu Z, Chen J, Danting Z, Han F and Ye S: tRNA derived fragment (tRF)-3009 participates in modulation of IFN-α-induced $CD4^+$ T cell oxidative phosphorylation in lupus patients. J Transl Med 19: 305, 2021.
16. Maute RL, Schneider C, Sumazin P, Holmes A, Califano A, Basso K and Dalla-Favera R: tRNA-derived microRNA modulates proliferation and the DNA damage response and is down-regulated in B cell lymphoma. Proc Natl Acad Sci USA 110: 1404-1409, 2013.
17. Ivanov P, O'Day E, Emara MM, Wagner G, Lieberman J and Anderson P: G-quadruplex structures contribute to the neuroprotective effects of angiogenin-induced tRNA fragments. Proc Natl Acad Sci USA 111: 18201-18206, 2014.
18. Chen Q, Yan M, Cao Z, Li X, Zhang Y, Shi J, Feng GH, Peng H, Zhang X, Zhang Y, *et al*: Sperm tsRNAs contribute to intergenerational inheritance of an acquired metabolic disorder. Science 351: 397-400, 2016.
19. Hogg MC, Raoof R, El Naggar H, Monsefi N, Delanty N, O'Brien DF, Bauer S, Rosenow F, Henshall DC and Prehn JH: Elevation in plasma tRNA fragments precede seizures in human epilepsy. J Clin Invest 129: 2946-2951, 2019.
20. Wang J, Han B, Yi Y, Wang Y, Zhang L, Jia H, Lv J, Yang X, Jiang D and Zhang J: Expression profiles and functional analysis of plasma tRNA-derived small RNAs in children with fulminant myocarditis. Epigenomics 13: 1057-1075, 2021.
21. Suh KS and Yuspa SH: Intracellular chloride channels: Critical mediators of cell viability and potential targets for cancer therapy. Curr Pharm Des 11: 2753-2764, 2005.
22. Fernández-Salas E, Suh KS, Speransky VV, Bowers WL, Levy JM, Adams T, Pathak KR, Edwards LE, Hayes DD, Cheng C, *et al*: mtCLIC/CLIC4, an organellular chloride channel protein, is increased by DNA damage and participates in the apoptotic response to p53. Mol Cell Biol 22: 3610-3620, 2002.
23. Suh KS, Mutoh M, Nagashima K, Fernandez-Salas E, Edwards LE, Hayes DD, Crutchley JM, Marin KG, Dumont RA, Levy JM, *et al*: The organellular chloride channel protein CLIC4/mtCLIC translocates to the nucleus in response to cellular stress and accelerates apoptosis. J Biol Chem 279: 4632-4641, 2004.
24. Abdul-Salam VB, Russomanno G, Chien-Nien C, Mahomed AS, Yates LA, Wilkins MR, Zhao L, Gierula M, Dubois O, Schaeper U, *et al*: CLIC4/Arf6 pathway. Circ Res 124: 52-65, 2019.
25. He G, Ma Y, Chou SY, Li H, Yang C, Chuang JZ, Sung CH and Ding A: Role of CLIC4 in the host innate responses to bacterial lipopolysaccharide. Eur J Immunol 41: 1221-1230, 2011.
26. Kleinjan ML, Mao Y, Naiche LA, Joshi JC, Gupta A, Jesse JJ, Shaye DD, Mehta D and Kitajewski J: CLIC4 regulates endothelial barrier control by mediating PAR1 signaling via RhoA. Arterioscler Thromb Vasc Biol 43: 1441-1454, 2023.
27. Livak KJ and Schmittgen TD: Analysis of relative gene expression data using real-time quantitative PCR and the 2(-Delta Delta C(T)) method. Methods 25: 402-408, 2001.
28. R Core Team: R: A Language and Environment for Statistical Computing. R Foundation for Statistical Computing, Vienna, Austria, 2023. https://www.R-project.org/.
29. Yeung ML, Bennasser Y, Watashi K, Le SY, Houzet L and Jeang KT: Pyrosequencing of small non-coding RNAs in HIV-1 infected cells: Evidence for the processing of a viral-cellular double-stranded RNA hybrid. Nucleic Acids Res 37: 6575-6586, 2009.
30. Martinez G, Choudury SG and Slotkin RK: tRNA-derived small RNAs target transposable element transcripts. Nucleic Acids Res 45: 5142-5152, 2017.
31. Matsui M and Corey DR: Non-coding RNAs as drug targets. Nat Rev Drug Discov 16: 167-179, 2017.
32. Tao EW, Wang HL, Cheng WY, Liu QQ, Chen YX and Gao QY: A specific tRNA half, 5'tiRNA-His-GTG, responds to hypoxia via the HIF1α/ANG axis and promotes colorectal cancer progression by regulating LATS2. J Exp Clin Cancer Res 40: 67, 2021.

33. Zong T, Yang Y, Lin X, Jiang S, Zhao H, Liu M, Meng Y, Li Y, Zhao L, Tang G, *et al*: 5'-tiRNA-Cys-GCA regulates VSMC proliferation and phenotypic transition by targeting STAT4 in aortic dissection. Mol Ther Nucleic Acids 26: 295-306, 2021.
34. Jehn J, Treml J, Wulsch S, Ottum B, Erb V, Hewel C, Kooijmans RN, Wester L, Fast I and Rosenkranz D: 5' tRNA halves are highly expressed in the primate hippocampus and might sequence-specifically regulate gene expression. RNA 26: 694-707, 2020.
35. Hang W, Chen C, Seubert JM and Wang DW: Fulminant myocarditis: A comprehensive review from etiology to treatments and outcomes. Signal Transduct Target Ther 5: 287, 2020.
36. Tao EW, Cheng WY, Li WL, Yu J and Gao QY: tiRNAs: A novel class of small noncoding RNAs that helps cells respond to stressors and plays roles in cancer progression. J Cell Physiol 235: 683-690, 2020.
37. Su Z, Kuscu C, Malik A, Shibata E and Dutta A: Angiogenin generates specific stress-induced tRNA halves and is not involved in tRF-3-mediated gene silencing. J Biol Chem 294: 16930-16941, 2019.
38. Fricker R, Brogli R, Luidalepp H, Wyss L, Fasnacht M, Joss O, Zywicki M, Helm M, Schneider A, Cristodero M and Polacek N: A tRNA half modulates translation as stress response in Trypanosoma brucei. Nat Commun 10: 118, 2019.
39. Li Q, Hu B, Hu GW, Chen CY, Niu X, Liu J, Zhou SM, Zhang CQ, Wang Y and Deng ZF: tRNA-derived small non-coding RNAs in response to ischemia inhibit angiogenesis. Sci Rep 6: 20850, 2016.
40. Pawar K, Shigematsu M, Sharbati S and Kirino Y: Infection-induced 5'-half molecules of tRNAHisGUG activate Toll-like receptor 7. PLoS Biol 18: e3000982, 2020.
41. Pekarsky Y, Balatti V, Palamarchuk A, Rizzotto L, Veneziano D, Nigita G, Rassenti LZ, Pass HI, Kipps TJ, Liu CG and Croce CM: Dysregulation of a family of short noncoding RNAs, tsRNAs, in human cancer. Proc Natl Acad Sci USA 113: 5071-5076, 2016.
42. Goodarzi H, Liu X, Nguyen HCB, Zhang S, Fish L and Tavazoie SF: Endogenous tRNA-derived fragments suppress breast cancer progression via YBX1 displacement. Cell 161: 790-802, 2015.
43. Sharma U, Conine CC, Shea JM, Boskovic A, Derr AG, Bing XY, Belleannee C, Kucukural A, Serra RW, Sun F, *et al*: Biogenesis and function of tRNA fragments during sperm maturation and fertilization in mammals. Science 351: 391-396, 2016.
44. Huang B, Yang H, Cheng X, Wang D, Fu S, Shen W, Zhang Q, Zhang L, Xue Z, Li Y, *et al*: tRF/miR-1280 suppresses stem cell-like cells and metastasis in colorectal cancer. Cancer Res 77: 3194-3206, 2017.
45. Boskovic A, Bing XY, Kaymak E and Rando OJ: Control of noncoding RNA production and histone levels by a 5' tRNA fragment. Genes Dev 34: 118-131, 2020.
46. Malik M, Jividen K, Padmakumar VC, Cataisson C, Li L, Lee J, Howard OM and Yuspa SH: Inducible NOS-induced chloride intracellular channel 4 (CLIC4) nuclear translocation regulates macrophage deactivation. Proc Natl Acad Sci USA 109: 6130-6135, 2012.